nature neuroscience

A tctex1-Ca^{2+} channel complex for selective surface expression of Ca^{2+} channels in neurons

Meizan Lai[1,5], Fushun Wang[5], Joyce G Rohan[2], Yuka Maeno-Hikichi[1,5], Yuan Chen[1,5], Yi Zhou[3], Guangping Gao[4], William A Sather[2] & Ji-fang Zhang[1,5]

Voltage-gated Ca^{2+} channels (VGCCs) are important in regulating a variety of cellular functions in neurons. It remains poorly understood how VGCCs with different functions are sorted within neurons. Here we show that the t-complex testis-expressed 1 (tctex1) protein, a light-chain subunit of the dynein motor complex, interacts directly and selectively with N- and P/Q-type Ca^{2+} channels, but not L-type Ca^{2+} channels. The interaction is insensitive to Ca^{2+}. Overexpression in hippocampal neurons of a channel fragment containing the binding domain for tctex1 significantly decreases the surface expression of endogenous N- and P/Q-type Ca^{2+} channels but not L-type Ca^{2+} channels, as determined by immunostaining. Furthermore, disruption of the tctex1–Ca^{2+} channel interaction significantly reduces the Ca^{2+} current density in hippocampal neurons. These results underscore the importance of the specific tctex1-channel interaction in determining sorting and trafficking of neuronal Ca^{2+} channels with different functionalities.

Multiple types of voltage-gated Ca^{2+} channels coexist in neurons and are pivotal in regulating a variety of cellular functions[1–3]. Studies have shown that different types of VGCCs are often associated with specific functions: release of neurotransmitter generally requires activation of N- and P/Q-type Ca^{2+} channels[2,4], whereas activation of L-type Ca^{2+} channels is implicated in such events as regulation of gene expression[5]. In accordance with their distinct functional roles, these Ca^{2+} channels show unique subcellular localizations in neurons. Immunocytochemical studies have found that L-type Ca^{2+} channels are primarily expressed in soma and proximal dendrites of many different types of neurons[6]. On the other hand, N- and P/Q-type Ca^{2+} channels can be found at the nerve terminal, in addition to the cell body[7,8].

Synaptogenesis is a dynamic process in the developing central nervous system (CNS) as well as in long-term synaptic plasticity[9,10]. Formation and maturation of functional synapses require rapid clustering and assembly of both presynaptic and postsynaptic elements. For instance, at glutamatergic synapses, hallmarks of mature synapses include clustering of postsynaptic density protein 95 (PSD-95) and assembly of glutamate receptors and other ion channels. So far, most studies of synaptogenesis have focused primarily on its postsynaptic elements, and molecular mechanisms responsible for sorting, trafficking, targeting and assembly of postsynaptic components have been identified[10,11]. In comparison, much less is known about molecular events underlying synaptogenesis at the presynaptic nerve terminal. There is emerging evidence that VGCCs are important in the formation of a mature and functional synapse. For instance, the laminin-VGCC interaction is essential for the formation of presynaptic active zones[12]. Through their interaction with the SNARE protein complex, VGCCs are an integral part of the synaptic vesicle release machinery[13], and as we have shown in a recent study, an essential part of the synaptic vesicle endocytosis machinery[14]. In addition, through protein-protein interactions, VGCCs may serve as anchors to bring synaptic vesicle release and recycling machineries into the presynaptic nerve terminal.

Despite the importance of VGCCs in many neuronal activities, the different subcellular localization of VGCCs with different functions is poorly understood[15]. Reports on targeting of VGCCs have relied exclusively on heterologous expression systems such as HEK293 cells, which do not necessarily resemble neurons (see references in ref. 15). For instance, a prominent feature of neurons is their polarity, with well-organized dendrites and axons; they require the microtubule system along with different motor proteins for anterograde and retrograde transport of various cellular components[16–19]. However, heterologous expression systems such as HEK293 cells do not have such a polarized and well-organized system. Thus, results of Ca^{2+} channel targeting from HEK 293 cells, although informative, may not reflect the real features in neurons.

Microtubule-based motor proteins, particularly kinesins, dyneins and myosins, are important in the transport of cellular organelles and protein complexes to various subcellular locations in neurons[16–19]. Evidence has emerged that microtubule motor proteins may

[1]Department of Pharmacology, University of Pennsylvania School of Medicine, 3620 Hamilton Walk, Philadelphia, Pennsylvania 19104, USA. [2]Department of Pharmacology, University of Colorado Health Sciences Center, P.O. Box 6511, Aurora, Colorado 80045, USA. [3]Department of Neurobiology, University of Alabama at Birmingham, 1719 6th Avenue South, Birmingham, Alabama 35294, USA. [4]Department of Molecular & Cellular Engineering, University of Pennsylvania School of Medicine, 3620 Hamilton Walk, Philadelphia, Pennsylvania 19104, USA. [5]Current addresses: Department of Physiology, Jefferson Medical College, 1020 Locust Street, Philadelphia, Pennsylvania 19107, USA (M.L., F.W., Y.C. and J.-f.Z.); Department of Physiology and Biophysics, Case Western Reserve University School of Medicine, Cleveland, Ohio 44106, USA (Y.M.-H.). Correspondence should be addressed to J.F.Z. (Ji-fang.Zhang@Jefferson.edu).

Published online 13 March 2005; doi:10.1038/nn1418

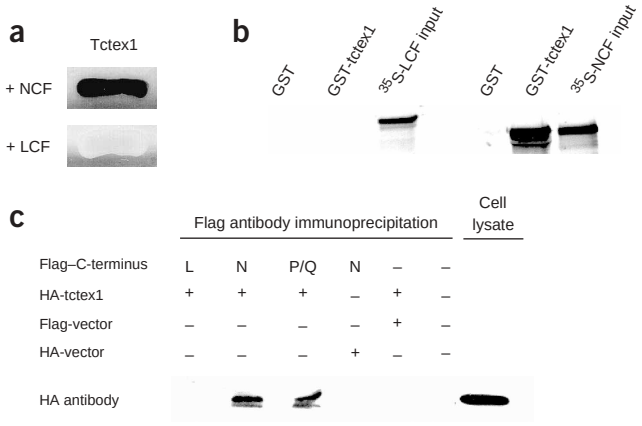

Figure 1 Selective interaction between tctex1 and N- and P/Q-type Ca^{2+} channels. (**a**) *lacZ* reporter gene assays in yeast. The full-length C terminus of N-type Ca^{2+} channels (NCF) or L-type Ca^{2+} channels (PCF) was transformed into yeast along with tctex1 and a *lacZ* reporter gene. Yeast transformed with NCF but not LCF turned blue. (**b**) GST fusion protein pulldown assay. Results are representative of at least three separate experiments. (**c**) Coimmunoprecipitation of tctex1 and C terminus of three different types of Ca^{2+} channels. HA-tagged tctex1 and Flag-tagged channel C termini were coexpressed in HEK 293 cells. CoIP assays were performed 2 d after transfection.

preferentially interact with specific cargoes to sort and traffic proteins of different functions within neurons. For example, formation of a macromolecular complex including kinesin and NR2B, an NMDA receptor subunit, specifies the dendritic distribution of NMDA receptors[20]. Direct interaction between tctex1 and rhodopsin is responsible for the unique distribution of rhodopsin in the outer segment of rod photoreceptors[21]. It is not known whether and which microtubule motors may contribute to the sorting of distinct VGCCs within neurons.

We addressed these questions by using yeast two-hybrid screening to identify the protein(s) that might contribute to sorting and trafficking of VGCCs in neurons. Biochemical studies show that tctex1, a light chain of the dynein motor complex, selectively interacts with N- and P/Q-type Ca^{2+} channels but not L-type Ca^{2+} channels. Formation of the tctex1–Ca^{2+} channel complex is not affected by different Ca^{2+} concentrations. Through mutagenesis, we have identified the tctex1 binding domain in the channel C terminus. When the tctex1 binding domain is overexpressed in hippocampal neurons as a dominant-negative construct, surface expression of endogenous N- and P/Q-type Ca^{2+} channels is markedly decreased, as shown by immunostaining. Furthermore, disruption of the tctex1–Ca^{2+} channel interaction by the dominant-negative construct significantly reduces the Ca^{2+} current density in hippocampal neurons. Our results demonstrate a unique role of tctex1 in sorting and trafficking of VGCCs with different functions within neurons.

Figure 2 Effects of Ca^{2+} on the tctex1-channel interaction, and identification of the tctex1 binding domain on the channel C terminus. (**a**) Ca^{2+} does not affect the interaction between tctex1 and NCF. Pulldown assays were performed at different Ca^{2+} concentrations as indicated. (**b**) Schematic representation of the channel α_1-subunit and its deletion mutations in the C terminus. Their interactions with tctex1 were tested using a yeast two-hybrid approach. (**c**) Verification of the interaction between tctex1 and deletion mutants by coimmunoprecipitation assays (WB, western blots).

RESULTS

Tctex1 binds selectively to N- and P/Q-type Ca^{2+} channels

To identify Ca^{2+} channel partner proteins that might contribute to sorting of VGCC subtypes to appropriate subcellular domains, we performed yeast two-hybrid screening of a rat brain cDNA library using as bait the full-length C termini of three different Ca^{2+} channel α_1-subunits: α_{1A} (CaV2.1, P/Q-type), α_{1B} (CaV2.2, N-type) and α_{1C} (CaV1.2, L-type)[14,22]. One clone, repeatedly pulled out by the C terminus of N-type Ca^{2+} channels (NCF), was identical to tctex1, a light chain subunit of the dynein motor protein complex[23]. Cytoplasmic dynein is a multimeric motor complex consisting of two heavy chains with motor domains, as well as several intermediate, light intermediate and light chains. Motor protein subunits, including dynein subunits, are key to determining subcellular distribution of specific organelles and protein complexes[17,18,24].

In yeast, we established the interaction between tctex1 and NCF through both a *lacZ* reporter gene assay (**Fig. 1a**) and galactose-dependent growth in leucine-deficient medium. In contrast to the N-type channel C terminus, tctex1 did not bind to L-type Ca^{2+} channel C termini (LCF) in yeast (**Fig. 1a**). We further tested the selective interaction between tctex1 and NCF through GST fusion protein pulldown assays. Similar to the results in yeast, GST-fused tctex1 interacted with only ^{35}S-labeled NCF, not ^{35}S-labeled LCF (**Fig. 1b**).

Multiple types of VGCCs are found in neurons, including L-, N- and P/Q-types[1–3]. We tested whether tctex1 could bind to P/Q-type Ca^{2+} channels, which, like N-type Ca^{2+} channels, are present in the presynaptic nerve terminal and support synaptic transmission[2,4]. We carried out coimmunoprecipitation (CoIP) assays using lysates from HEK 293 cells coexpressing tctex1 and the C terminus of L-, N- or P/Q-type channels. Consistent with the results of *in vitro* assays, tctex1 interacted with the C terminus of the N-type channel but the not L-type channel (**Fig. 1c**). In addition, tctex1 bound to the C terminus of P/Q-type channels. Thus, tctex1 can selectively bind to both N- and P/Q-type Ca^{2+} channels, which are localized at the nerve terminal for release of neurotransmitters, but not to L-type Ca^{2+} channels, which

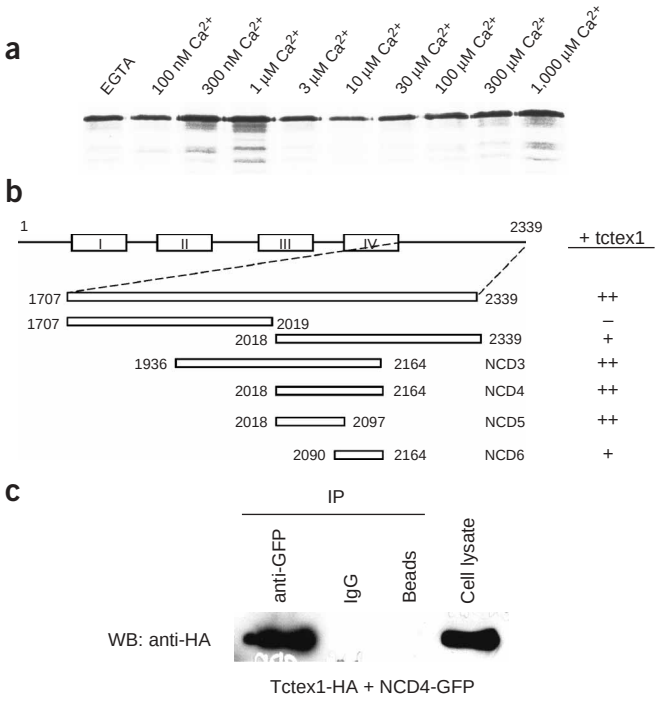

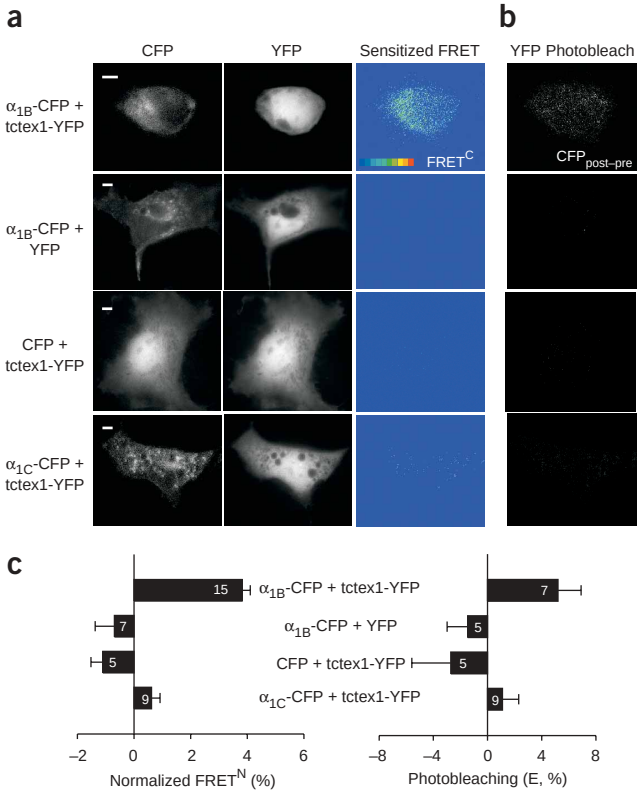

Figure 3 Sensitized FRET and acceptor photobleaching measurements point to interaction between tctex1 and full-length N-type Ca^{2+} channels. (**a**) Sets of CFP, YFP and corrected, sensitized FRET images for four representative COS-7 cells transfected with various pairs of CFP- and YFP-bearing constructs. *FRET*^{C} was present between tctex1 and the N-type Ca^{2+} channel subunit α_{1B}. In the negative control experiments, little or no *FRET*^{C} was detectable between α_{1B} and free YFP, between tctex1 and free CFP, or between tctex1 and α_{1C}. Intensity scale = 0 (blue) to 40 (red), arbitrary units. Scale bars, 5 μm. (**b**) Donor dequenching via acceptor photobleaching also shows interaction between tctex1 and the N-type Ca^{2+} channel, but not between the other fluorescent partners presented. (**c**) Summary bar graphs showing average, normalized *FRET*^{C} and FRET efficiency (*E*, %) obtained from donor dequenching. White numbers in the bar graph indicate the number of cells used for FRET measurements.

are found primarily on the cell body. This conclusion was further strengthened by the results of functional studies (discussed below).

In neurons, local Ca^{2+} concentrations near VGCCs change markedly, from the resting level of approximately 100 nM to 200–300 μM when VGCCs are activated by an action potential[25]. In a recent study, we have shown that Ca^{2+} can regulate formation of the endophilin-Ca^{2+} channel complex through a previously unknown Ca^{2+} sensor[14]. Such a Ca^{2+}-dependent interaction may provide a mechanism for Ca^{2+} to regulate synaptic vesicle endocytosis. To test whether changes in Ca^{2+} concentrations might affect the interaction between tctex1 and N-type Ca^{2+} channels, we performed GST fusion protein pulldown assays at different Ca^{2+} concentrations, ranging from 0 (in the presence of EGTA) to 1 mM. Tctex1 remained channel-bound regardless of the Ca^{2+} concentrations, suggesting that changes in Ca^{2+} concentrations do not appreciably change the affinity of tctex1 for N-type Ca^{2+} channels (**Fig. 2a**). This Ca^{2+}-independent interaction differs from the interaction between Ca^{2+} channels and other partner proteins such as endophilin[14]. It is not unexpected that binding of tctex1 to N-type Ca^{2+} channels is insensitive to Ca^{2+}, based on the functional consequence of the interaction (see below) and the absence of known Ca^{2+}-binding domains within the tctex1 amino acid sequence.

We next sought to identify the tctex1 binding domain within the channel C terminus. We generated a series of channel deletion mutants and evaluated their abilities to bind to tctex1 by the yeast two-hybrid approach (**Fig. 2b**). The tctex1 binding domain was mapped to a segment corresponding to amino acid residues 2018–2097 of the N-type channel α_1 subunit (NCD5, **Fig. 2b**). This segment is located upstream of an alternative splicing site that generates two isoforms of α_{1B}-subunits[26], indicating that tctex1 can bind to both isoforms of N-type Ca^{2+} channels. We verified the results from deletion mutations through approaches independent of yeast; for example, using GFP-tagged NCD4 immunoprecipitated hemagglutinin (HA)-tagged tctex1 (**Fig. 2c**). The existence of a unique tctex1 binding domain in NCF provides another piece of evidence supporting the specific interaction between tctex1 and the Ca^{2+} channel. The deletion mutant NCD4, which encompasses the tctex1 binding domain (**Fig. 2b**), provided a useful tool for functional studies (see below).

Formation of a tctex1–Ca^{2+} channel complex *in vivo*

We then investigated whether tctex1 and the full-length N-type Ca^{2+} channel could form macromolecular complexes in living cells by measuring fluorescence resonance energy transfer (FRET) between fluorescently labeled tctex1 and Ca^{2+} channel constructs. Yellow fluorescent protein (YFP)-tagged tctex1 was coexpressed with the cyan fluorescent protein (CFP)-tagged N-type Ca^{2+} channel α_1-subunit (α_{1B}) in COS-7 cells. CFP-tagged L-type Ca^{2+} channels (α_{1C}) served as a negative control. Two methods, sensitized FRET and donor dequenching via acceptor photobleaching, were used to provide complementary estimates of FRET between the CFP- and YFP-tagged constructs[27–29]. With both methods, coexpression of fluorescently labeled tctex1 and L-type Ca^{2+} channels did not produce FRET (**Figs. 3a,b**), indicating that in living cells, tctex1 was not in close proximity to L-type Ca^{2+} channels. In sharp contrast, coexpression of tctex1 and full-length N-type Ca^{2+} channels produced significantly greater FRET than did coexpression of tctex1 and L-type Ca^{2+} channels (3.82 ± 0.29 versus 0.62 ± 0.30 for normalized FRET, $P < 0.001$; 5.2 ± 1.7 versus 1.1 ± 1.2 for E (%), $P = 0.028$, **Fig. 3c**). The FRET efficiency between tctex1 and N-type channels was comparable to that between calmodulin and P/Q-type Ca^{2+} channels[30]. These results provide direct evidence that, in living cells, tctex1 selectively associates with functional N-type Ca^{2+} channels.

We carried out CoIP assays to further explore whether the tctex1-channel complex existed *in vivo*, using lysate prepared from the adult

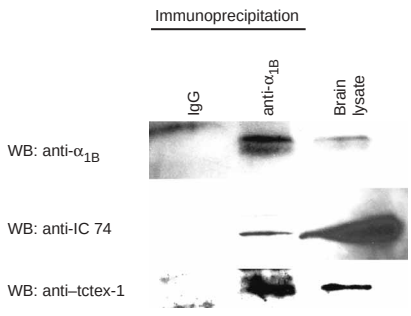

Figure 4 Formation of the tctex1–Ca^{2+} channel complex *in vivo*. CoIP assays, using brain lysate, were performed using antibody against N-type Ca^{2+} channels immunoprecipitation and probed with different antibodies as indicated.

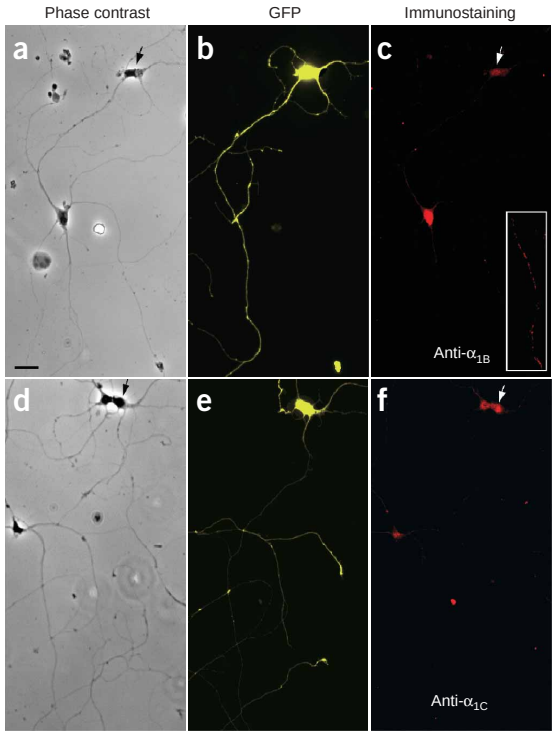

Figure 5 Overexpression of a dominant-negative construct, NCD4-GFP, reduces surface expression of endogenous N-type Ca^{2+} channels. (**a**,**d**) DIC images of transfected (arrow) and non-transfected neurons. Scale bars, 25 μm. (**b**,**e**) GFP images of transfected neurons. (**c**,**f**) Immunofluorescent images of the same neurons stained with antibodies as indicated. Arrows indicate transfected neurons.

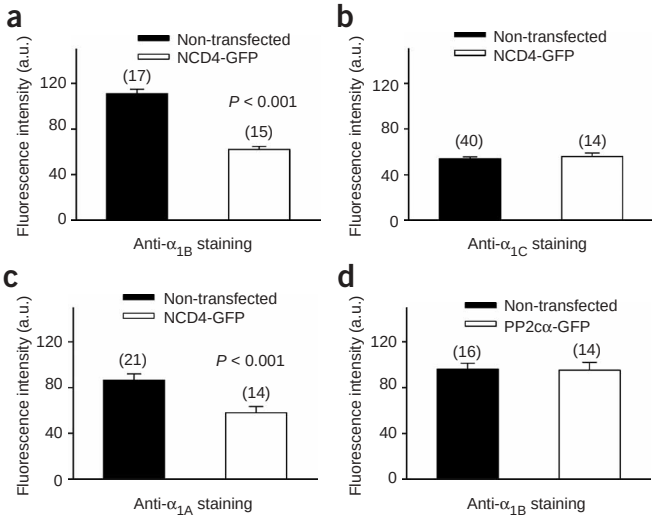

Figure 6 Quantitative summary of the effects of overexpression of a dominant-negative construct on surface expression of three different types of endogenous Ca^{2+} channels. (**a**) NCD4 reduces surface expression of endogenous N-type Ca^{2+} channels. (**b**) Endogenous L-type Ca^{2+} channel expression is not affected by NCD4. (**c**) Endogenous P/Q-type Ca^{2+} channel expression is reduced by NCD4. (**d**) Overexpression of a phosphatase does not alter expression of endogenous N-type Ca^{2+} channels. Values in parentheses indicate number of transfected or non-transfected neurons from at least three different transfections.

rat brain. Consistent with the *in vitro* data obtained using expressed Ca^{2+} channel C termini and with the FRET data, antibody to α_{1B} (anti-α_{1B}) precipitated tctex1 from the crude membrane fraction of the brain preparation (**Fig. 4**). CoIP using HEK cells coexpressing tctex1 and N-type Ca^{2+} channels yielded the same results (data not shown). To determine whether Ca^{2+} channels might be associated with the dynein motor complex, of which tctex1 is a subunit, we investigated whether other dynein subunits could be detected in CoIP assays. Immunoblotting using antibody against a 74-kDa dynein intermediate chain was positive. These results, together with mutagenesis and functional studies (**Fig. 2** and below), show that tctex1 and Ca^{2+} channels form a functional complex *in vivo*.

Dominant-negative construct on channel expression *in vivo*

As motor proteins are essential for transport of a variety of cellular organelles and protein complexes to various subcellular localizations[16–19], the tctex1-Ca^{2+} channel complex may play a role in transport of VGCCs. We sought to test whether overexpression of a dominant-negative construct could interfere with the tctex1–Ca^{2+} channel interaction and consequently the surface expression of Ca^{2+} channels in neurons. Our rationale was that overexpression of the tctex1 binding domain from Ca^{2+} channels would compete with and therefore displace the endogenous N- and P/Q-type Ca^{2+} channels for binding to endogenous tctex1. As a result, the surface expression of the endogenous N- and P/Q-type Ca^{2+} channels could be altered in the transfected neurons.

Mutagenesis studies showed that the tctex1 binding domain in the Ca^{2+} channel C terminus was located within a fragment of 140 amino acid residues (NCD4, **Fig. 2c**). BLAST searching of the GenBank database with this fragment did not pick up any other proteins except the N-type Ca^{2+} channel itself, indicating that it was not likely that overexpression of NCD4 would interfere with other signaling processes in neurons. GFP-tagged NCD4 was transfected into hippocampal neurons at 6 d *in vitro* (DIV) and neurons were fixed for immunostaining with channel-specific antibodies at 12 DIV, when cultured hippocampal neurons are fully developed and functional synapses are formed[31,32]. Quantitative comparisons of immunofluorescence intensity were made between transfected neurons and neighboring non-transfected neurons on the same coverslip. Such comparisons minimized the inherent variation of immunostaining among different batches of samples.

Immunostaining of non-transfected hippocampal neurons with antibodies against Ca^{2+} channels displayed diffuse staining of L- and N-type Ca^{2+} channels throughout the soma and apical dendrites, suggesting that mature hippocampal neurons expressed both L- and N-type Ca^{2+} channels on the cell body (**Fig. 5**). This was consistent with previous studies using immunostaining or electrophysiological recordings[33–35]. Non-transfected mature hippocampal neurons also showed punctate staining of N-type Ca^{2+} channels along the axons (**Fig. 5c**, inset). Identification of axons by morphology was confirmed by immunostaining with an antibody against MAP2 (data not shown)[31,32]. Immunostaining of P/Q-type Ca^{2+} channels yielded results similar to those for N-type Ca^{2+} channels (data not shown).

Morphology of neurons transfected with GFP-tagged NCD4 was similar to morphology of non-transfected control neurons, with well-developed dendrites and axons (**Figs. 5a,d**), and Ca^{2+} currents could be recorded. When overexpressed, NCD4-GFP was evenly distributed throughout the entire neuron (**Figs. 5b,e**). However, for neurons transfected with NCD4-GFP, cell surface expression of endogenous N-type Ca^{2+} channels was significantly lower (**Fig. 5b**). On average, the

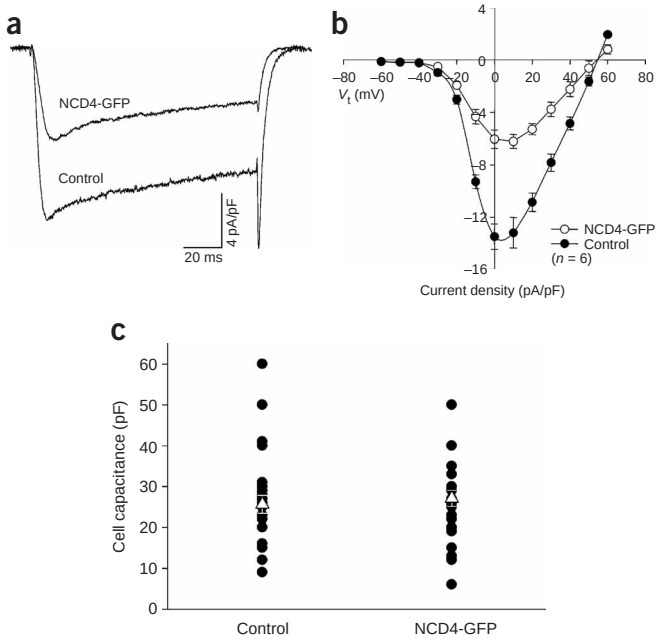

Figure 7 Disruption of the tctex1–Ca^{2+} channel interaction reduces the Ca^{2+} current density in hippocampal neurons. (**a**) Exemplar current traces obtained from a non-transfected neuron and a neuron transfected with NCD4-GFP. The holding potential was –70 mV and the test potential was 0 mV. (**b**) *I-V* curves from control and NCD4-transfected neurons. Peak currents were normalized to the cell capacitance. (**c**) Cell capacitance of control and NCD4-transfected neurons. Filled circles, capacitance of individual neurons; open triangles, mean values of the capacitance. For NCD4-tranfected neurons, capacitance from different time groups was pooled.

fluorescence intensity for N-type Ca^{2+} channels on the cell body was almost 50% lower, from 110.85 ± 3.85 to 62.17 ± 2.61 (arbitrary units, a.u., mean ± s.e.m., $P < 0.001$, **Fig. 6a**). The punctate staining of N-type Ca^{2+} channels on axons was also lower or even undetectable. In contrast, immunostaining of L-type Ca^{2+} channels was similar in transfected and non-transfected neurons (**Fig. 5f**). Quantitative analysis showed that cell surface expression of endogenous L-type Ca^{2+} channels was not affected by transfection of NCD4-GFP (**Fig. 6b**). On the other hand, surface expression of P/Q-type Ca^{2+} channels, which interacted with tctex1 (**Fig. 1c**), was significantly reduced by NCD4-GFP in the transfected neurons (from 86.48 ± 5.34 to 58.04 ± 5.58, $P < 0.001$, **Fig. 6c**).

Several lines of evidence suggested that the lower surface expression of endogenous N- and P/Q-type Ca^{2+} channels in transfected neurons could not be attributed to experimental artifacts. First, surface expression of endogenous L-type Ca^{2+} channels, which did not bind to tctex1 (**Fig. 1**), was not affected by overexpression of NCD4-GFP (**Figs. 5f** and **6b**). Second, we overexpressed three unrelated proteins as well as a fragment from the C terminus of the L-type Ca^{2+} channel α_1-subunit, none of which affected the surface expression of endogenous N-type Ca^{2+} channels in hippocampal neurons. For example, overexpression of a GFP-tagged phosphatase had no effects on surface expression of endogenous N-type Ca^{2+} channels (**Fig. 6d**). Third, two different kinds of antibodies to α_{1B} were used, both yielding the same results.

Overexpression of NCD4 reduces the Ca^{2+} current density

Electrophysiological recordings were carried out to further test the effects of NCD4 on cell surface expression of endogenous Ca^{2+} channels in transfected hippocampal neurons. Nifedipine (1 μM) was included in the bath solution to block L-type Ca^{2+} channels. Under this condition, the primary Ca^{2+} current component should be of N- and P/Q-type with a very small percentage of R-type Ca^{2+} current[3]. Forty-eight hours after transfection, the Ca^{2+} current density was substantially lower in NCD4-GFP–transfected neurons than in non-transfected neurons (**Fig. 7a**). On average, the Ca^{2+} current density was reduced by more than 50%, from 14.6 ± 1.01 pA pF^{-1} to 7.0 ± 0.69 pA pF^{-1} ($V_t = 0$ mV, $P < 0.001$). Transfection of NCD4-GFP did not affect voltage-dependent activation of the Ca^{2+} currents (**Fig. 7b**). Reduction of the Ca^{2+} current density by NCD4-GFP was observed at all the test voltages. Transient expression of NCD4-GFP did not alter the size of the transfected neurons, as the cell capacitance was identical in transfected (27.1 ± 1.97 pF, $n = 27$) and non-transfected neurons (25.6 ± 2.18 pF, $n = 27$, $P > 0.6$, **Fig. 7c**). This result rules out changes in cell size as a potential contributing factor for the reduced Ca^{2+} current density.

After transfection, the effects of NCD4 increased with time. Reduction of the Ca^{2+} current density in the NDC4-GFP–transfected neurons was significant 24 h after transfection (8.8 ± 0.73 pA pF^{-1}, $n = 7$, $P = 0.0072$). The Ca^{2+} current density was further reduced to 7.0 ± 0.69 pA pF^{-1} and 6.0 ± 0.67 pA pF^{-1} at 48 and 72 h after transfection, respectively (**Fig. 8a**). To further test the specificity of the effects of NCD4-GFP, we transfected neurons with GFP alone or

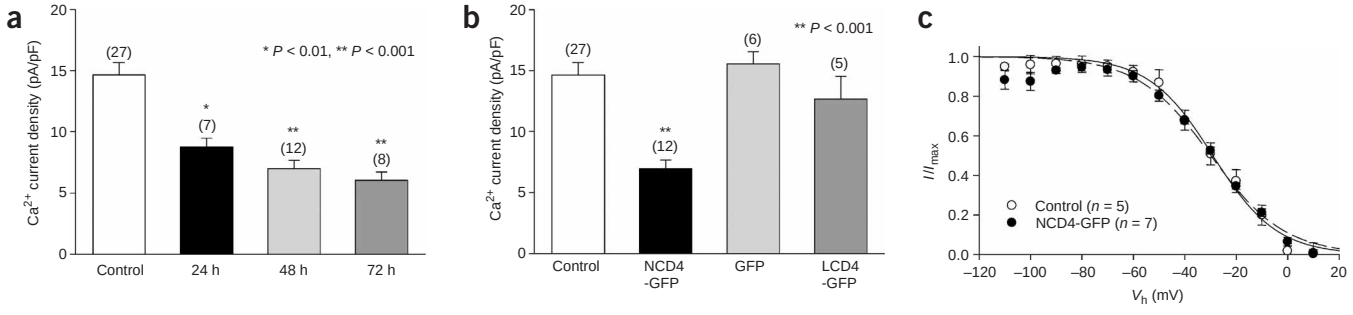

Figure 8 Quantitative analysis of the effects of NCD4-GFP on the Ca^{2+} current density in hippocampal neurons. (**a**) Reduction of the Ca^{2+} current density by NCD4-GFP with time. Values in parentheses indicate number of transfected or non-transfected neurons from at least three different transfections. (**b**) Summary of the effects of different constructs on the Ca^{2+} current density 48 h after their transfection in hippocampal neurons ($V_t = 0$ mV, and $V_h = -70$ mV). (**c**) Overexpression of NCD4-GFP does not shift the steady-state inactivation curves. Peak Ca^{2+} currents obtained at different holding potentials were normalized to the maximal value and fit to the Boltzmann equation.

GFP-tagged LCD4, a counterpart fragment from the L-type Ca^{2+} channel C terminus with 10% homology to NCD4 in its primary amino acid sequence. Overexpression of both constructs in hippocampal neurons did not have any significant impact on the Ca^{2+} current density (**Fig. 8b**). We next examined whether expression of NCD4-GFP affected the steady-state inactivation of the Ca^{2+} current. A shift in the steady-state inactivation by NCD4 could result, in principle, in reduction of the Ca^{2+} current density, when Ca^{2+} currents were elicited at the same holding potential. Analysis showed that the midpoint of the steady-state inactivation curves remained the same for control (-32.2 ± 2.86 mV, $n = 5$) and NCD4-transfected (-29.8 ± 3.14 mV, $n = 7$) neurons (**Fig. 8c**). Taken together, the electrophysiology data are consistent with the immunostaining data and suggest that formation of the tctex1–Ca^{2+} channel complex is responsible for surface expression of functional N- and P/Q-type Ca^{2+} channels in neurons.

DISCUSSION

Increasing evidence shows that selective interactions between motor protein subunits and their specific cargoes determine the subcellular distribution of proteins with different functionalities[18,24]. Our results demonstrate that selective interactions between tctex1 and N- and P/Q-type Ca^{2+} channels are important in determining the surface expression of these two types of Ca^{2+} channels in hippocampal neurons. Overexpression of a dominant-negative construct can effectively reduce the surface expression of both N- and P/Q-type Ca^{2+} channels, as measured by immunostaining as well as in electrophysiological recordings. L-type Ca^{2+} channels, on the other hand, do not bind to tctex1, and their surface expression is not affected by the dominant-negative construct. The functional role of the tctex1-channel complex is reminiscent of the interaction between the kinesin motor protein and NR2B for dendritic distribution of NMDA receptors in neurons[20].

Neurons express multiple types of VGCCs, which are associated with specific cellular functions[1–3]. These different types of Ca^{2+} channels have distinct subcellular localizations[6–8]. Whereas the L-type Ca^{2+} channel C terminus does not interact with tctex1, it did pull out a different motor protein, a member of the kinesin superfamily, during our yeast two-hybrid screening (Y.M.H. and J.F.Z., unpublished data). Molecular motors of the kinesin superfamily are responsible for the dendritic distribution of NMDA receptors[20]. As L- and N-type Ca^{2+} channels have different subcellular locations and different roles in cellular signaling[5,6], their preferential interactions with different motor proteins may provide molecular mechanisms for unique subcellular distributions of different Ca^{2+} channels.

Channel targeting to a specific subcellular localization includes at least two processes: transport of the newly synthesized channel from endoplasmic reticulum and Golgi apparatus to the final destination, and anchoring of the channel at the destination. One likely interpretation is that tctex1 plays a role in the transport process, because anchoring of N-type Ca^{2+} channels at the presynaptic nerve terminal requires additional partner proteins, notably the synaptically localized adaptor proteins Mint1 and CASK[36]. The binding site on the channel C terminus for Mint1 and CASK is located downstream of the tctex1 binding site. Thus, specific interactions between Ca^{2+} channels and their selective partner proteins have a unique role in determining the subcellular localizations of different types of VGCCs in neurons.

Dynein is a multimeric complex: in addition to its two main motor domains, there are several additional tightly associated subunits, including light intermediate chains (DLIC), intermediate chains (DIC) and light chains (DLC)[17–19,37]. These subunits and their isoforms can bind to distinct cargoes to transport specific cellular organelles and protein complexes. A growing list of tctex1 cargo proteins includes rhodopsin, gephyrin, voltage-dependent anion channels, doc2, fyn kinase and Trk neurotrophin receptors[21,38–42]. In our case, tctex1 binds selectively to N- and P/Q-type, but not L-type, Ca^{2+} channels. Thus, tctex1 does not transport a specific cargo protein but rather a subset of cargoes. It will be interesting to determine the molecular mechanism(s) by which tctex1 selectively binds to its specific cargoes, and particularly whether a common tctex1-binding domain exists in these cargo proteins. A recent study suggested that the tctex1 binding domain included a motif of (R/K)(R/K)XX(R/K)[43]. However, both L- and N-type Ca^{2+} channel C termini have this motif but show preferential binding to tctex1. The L-type Ca^{2+} channel C terminus does not bind to tctex1 (**Fig. 1**), indicating that additional structural factors may determine whether tctex1 binds to its selected cargoes.

The dynein complex is generally thought to be a minus-end–directed molecular motor, primarily responsible for fast retrograde transport along the axon to the cell body[17,18,44]. This mechanism, however, will not move VGCCs from the cell body to the nerve terminal, although it may be involved in retrograde transport of VGCCs for recycling. Electrophysiological recordings show that the Ca^{2+} current density is reduced by 40% 24 h after transfection of the dominant-negative construct in neurons. It is not likely that such a substantial reduction of the current density is due exclusively to impaired retrograde transport of VGCCs from the nerve terminals. Assuming tctex1 acts only as a part of the dynein complex, our results suggest other functions of the dynein motor complex in addition to fast retrograde transport. Indeed, as summarized in a recent review, in addition to fast retrograde transport, the dynein motor complex is involved in axonal transport such as slow anterograde transport[16]. Genetic defects in the dynein motor have been implicated in neurodegeneration. However, the morphological abnormalities can not be accounted for by defective retrograde transport alone[16]. Thus, the roles of the dynein complex in axonal transport are more complicated than previously thought. It remains to be tested whether the dynein motor complex itself is directly involved in surface expression of N- and P/Q-type Ca^{2+} channels *in vivo*.

Alternatively, it is possible that tctex1 may act independently of the dynein motor complex and the microtubule system. For instance, formation of the tctex1-channel complex may contribute to the transport of newly synthesized Ca^{2+} channels out of the Golgi apparatus, where tctex1 is known to exist[45]. This might explain the observation that 24 h after transfection of the dominant-negative construct, the marked reduction in Ca^{2+} current density could not be detected by immunostaining. In this case, the results of immunostaining, measured as the average fluorescence intensity on the cell body, might include signals from Ca^{2+} channels in the Golgi apparatus in addition to channels in the cell plasma membrane. Electrophysiological recordings, on the other hand, only measured the Ca^{2+} channels in the plasma membrane. Formation of the tctex1-channel complex may also contribute to anchoring of Ca^{2+} channels, as electron microscopic studies show that tctex1 is enriched in the presynaptic nerve terminal but not in postsynaptic elements[46]. It is generally thought that the microtubule system does not exist in the presynaptic nerve terminal, suggesting that tctex1 may function independently of the microtubule system in the nerve terminal.

VGCCs are a key component at the presynaptic nerve terminal for maturation of the functional synapses as well as for release of neurotransmitters. The laminin-VGCC interaction is essential for formation of presynaptic active zones[12]. Through their interaction with the SNARE protein complex, VGCCs serve to anchor the synaptic vesicle release machinery at the presynaptic boutons[13]. Ca^{2+} influx through VGCCs is key in regulating fast synaptic vesicle exocytosis and

endocytosis[13,47–49]. As well as interacting with Ca^{2+} channels, tctex1 is known to interact with doc2, which has been implicated as part of the synaptic vesicle release machinery[40,50]. Thus, tctex1 may be important in synaptogenesis and synaptic plasticity.

METHODS

Yeast two-hybrid screening. Details of screening can be found elsewhere[22]. The C terminus of the α_{1A} (CaV2.1, amino acid residues 1819–2422), α_{1B} (CaV2.2, aa 1707–2339) or α_{1C} (CaV1.2, aa 1505–2171) subunits was used as bait to screen a rat brain cDNA library (OriGene). Approximately 7×10^6 to 1×10^8 independent clones were screened for each bait. Over 200 clones were identified out of approximately 2,000 positive clones.

Construction and expression of recombinant proteins. A PCR-based method was used to generate the constructs, which were verified by sequencing. To generate recombinant proteins, cDNA constructs were subcloned into pGEX-4T-1 (Pharmacia) for GST-fused proteins. GST fusion proteins were produced in *Escherichia coli* and purified with glutathione-conjugated agarose beads (Pharmacia). To express the recombinant proteins in mammalian cells, cDNA constructs were subcloned into HA-tagged pcDNA 3, FLAG-tagged pcDNA 3 or pEGFP (Clontech). The calcium phosphate method was used for transfection in HEK 293 cells or hippocampal neurons.

For FRET measurements, cDNAs encoding Ca^{2+} channel α_{1B} (N-type) and α_{1C} (L-type) were subcloned into the pECFP-N1 vector (Clontech). Tctex1 was subcloned into pEYFP-N1 (Clontech). An equimolar ratio of cDNAs encoding Ca^{2+} channel subunits α_{1B}-CFP or α_{1C}-CFP, β_3, $\alpha_2\delta$ and tctex1-YFP were transiently transfected into COS-7 cells using the Effectene transfection reagent (Qiagen).

GST fusion protein pulldown assays. Pulldown assays were carried out as previously described[22]. Briefly, an ^{35}S-labeled C-terminal fragment of the α_{1B} subunit was synthesized using an *in vitro* protein translation kit (Promega). The assay buffer contained 100 mM NaCl, 20 mM Tris-HCl and 5% glycerol (pH 7.0) along with 1% Triton X-100 and a cocktail of protease inhibitors. Approximately 5 μg of GST-fused protein was incubated with 2 μl of ^{35}S-labeled NCF at 4 °C with gentle rocking. The length of incubation varied from 2 h to 12 h. The results were analyzed by SDS-PAGE and autoradiography. Typically, 0.5 μl of ^{35}S-labeled protein was used as input on the gel.

Coimmunoprecipitation and immunoblotting. Coimmunoprecipitations of tctex1 and calcium-channel C termini were performed using adult rat cortical extracts or cell lysates prepared from HEK 293 cells coexpressing tctex1 and the various channel C-terminal constructs as previously described[14,22]. Briefly, the soluble membrane fraction of adult rat cortical extracts was incubated for 10 to 12 h at 4 °C with anti-α_{1B} (Alomone Labs) conjugated to protein G–Sepharose beads. The immunoprecipitation buffer contained (in mM): 137 NaCl, 2.7 KCl, 4.3 Na_2HPO_4, 1.4 KH_2PO_4, 5 EGTA and 5 EDTA (pH 7.5). Immune complexes were resolved by SDS-PAGE and analyzed by immunoblotting with antibodies against the 74-kDa intermediate chain of the dynein motor complex (Santa Cruz) and α_{1B}.

Cell cultures. Animal use was approved by the University of Pennsylvania and Jefferson Medical College institutional animal care and use committees. Briefly, hippocampal neurons were prepared from E18–E19 embryonic rats (Sprague-Dawley). The medium was Neurobasal medium supplemented with 10% fetal bovine serum and B-27 and aerated with 5% CO_2. For electrophysiology experiments, cultured neurons were transfected with different cDNA constructs on 10 DIV and physiology experiments were performed on 12 DIV. HEK 293T and COS-7 cells were maintained under 5% CO_2 at 37 °C and in DMEM medium supplemented with 10% FBS, 100 U ml^{-1} penicillin and 0.1 mg ml^{-1} streptomycin.

Immunocytochemistry. Hippocampal neurons were fixed with 4% paraformaldehyde and 4% sucrose in PBS for 10 min, permeabilized with 0.25% Triton X-100 in PBS for 5 min, and quenched with 0.1 M glycine in PBS. The following primary antibodies were used at the indicated concentration: anti-α_{1A} (1:200, Alomone Labs), anti-α_{1B} A (1:200, Alomone Labs), anti-α_{1B} B (1:200), anti-α_{1C} (1:200, Alomone Labs) and anti-MAP2 (Sigma, 1:1000). FITC- (Jackson Labs), rhodamine- (Jackson Labs) or Alexa 568–conjugated (Molecular Probes) secondary antibodies were used for visualization. Fluorescent images were collected with a Nikon Eclipse TE200 inverted microscope. Cell surface fluorescence intensity was quantified with NIH Image software. Student's *t*-test was used for statistical comparisons. Unless otherwise stated, cultured neurons were transfected with different constructs at 6 DIV and fixed for immunostaining at 12 DIV.

Fluorescence resonance energy transfer (FRET) measurement. As described elsewhere in detail[27,28], fluorescence images were acquired 2–3 d after transfection using a Nikon inverted microscope equipped with a 175 W Xenon power source, 60× oil-immersion objective lens, 16 MHz CCD camera (SensiCam QE) and dual filter wheels that were controlled by SlideBook 3.0 software (Intelligent Imaging Innovation). Transfected COS-7 cells were bathed in a solution containing (in mM): 125 NaCl, 1 $CaCl_2$, 10 HEPES and 20 sucrose (pH 7.3). For sensitized FRET measurements (corrected FRET ($FRET^C$)), sets of three images were captured (200-ms exposures) using three different filter sets and an 86004BS dichroic mirror (Chroma): the donor (*D*; CFP) filter set (436 center excitation wavelength and 10 nm bandwidth (436/10 nm), emission 470/30 nm), the acceptor (*A*; YFP) filter set (excitation 500/20 nm, emission 535/30 nm), and the FRET (*F*) filter set (excitation 436/10 nm, emission 535/30 nm). All acquired images were background-subtracted pixel by pixel, using images of fields containing no cells. In addition, raw FRET images obtained with the FRET filter set were corrected for contamination by two non-FRET components: CFP emission bleeding through the emission filter in the FRET filter set, and direct excitation of YFP by light used to excite CFP. These two bleedthrough components were subtracted pixel by pixel from the raw images, using the following equation[27]: $FRET^C = F_{D,A} - (F_D/D_D) \times D_{D,A} - (F_A/A_A) \times A_{D,A}$. $F_{D,A}$ is the uncorrected, raw FRET image obtained with the FRET filter set (F) when both donor (CFP) and acceptor (YFP) are present, and $D_{D,A}$ and $A_{D,A}$ are the images obtained from the identical field of view using the donor (D) and acceptor (A) filter sets, respectively. Using cells transfected with donor alone, bleed of donor signal through the FRET emission filter relative to donor signal through the donor emission filter was measured ($F_D/D_D = 0.50$). Using cells transfected with acceptor alone, the relative error due to direct excitation of acceptor by light used to excite donor was measured ($F_A/A_A = 0.015$). To normalize for differences between cells in expression levels, $FRET^C$ calculations were divided by the square root of the product of CFP and YFP fluorescence.

Acceptor photobleaching (donor dequenching) was carried out by photobleaching YFP with 1-min continuous excitation through the YFP filter. CFP emission was measured before (D_{pre}) and after (D_{post}) photobleaching of YFP, and FRET efficiency[29] was calculated as $E\ (\%) = [1–(D_{PRE}/D_{POST})] \times 100$. Values were expressed as mean ± s.e.m.

Electrophysiological recordings. Briefly, whole cell recordings were obtained using an Axopatch 200B amplifier (Axon Instruments). Axon pClamp 8.0 software was used for data acquisition and analysis. Leak currents and capacitive transients were subtracted, online, with a P/4 protocol. The bath solution was composed of (in mM): 128 NaCl, 5 KCl, 5 $BaCl_2$, 1 $MgCl_2$, 10 HEPES, 10 TEA-Cl, and 10 glucose (pH = 7.3). Tetrodotoxin (500 nM, Alomone Labs) and nifedipine (1 μM, Calbiochem) were added in the bath solution to block Na^+ and L-type Ca^{2+} channels. Under these conditions, the primary Ca^{2+} current component was N- and P/Q-type, with a very small percentage of R-type Ca^{2+} current[3]. The recording pipette was filled with a solution containing (in mM) 108 CsCl, 4.5 $MgCl_2$, 10 EGTA, 25 HEPES, 4 ATP and 0.3 GTP (pH = 7.2). Current records were digitized at 10 kHz and low-pass filtered at 1 kHz.

Accession numbers. Accession numbers (GenBank) for the clones used in this study are X57477 for α_{1A} (CaV2.1), M94172 for α_{1B} (CaV2.2), X15539 for α_{1C} (CaV1.2) and NM_031318 for tctex1.

ACKNOWLEDGMENTS

We thank R. Pittman for the use of a Nikon Eclipse TE2000 inverted microscope; K. Campbell and C.H. Sung for anti-tctex1 antibody; M. Maronski and M. Dichter for help with hippocampal neuron cultures; P. Baas, K. Pfister and J. Meinkoth for helpful discussions and comments; and J. Field for initial help

with yeast two-hybrid screening. This work was supported by grants from the US National Institutes of Health (J.F.Z. & W.A.S.), the American Heart Association (J.F.Z.) and the National Alliance for Research on Schizophrenia and Depression (Y.M.H.).

COMPETING INTERESTS STATEMENT

The authors declare that they have no competing financial interests.

Received 17 November 2004; accepted 8 February 2005
Published online at http://www.nature.com/natureneuroscience/

1. Catterall, W.A. Structure and function of neuronal Ca^{2+} channels and their role in neurotransmitter release. *Cell Calcium* **24**, 307–323 (1998).
2. Dunlap, K., Luebke, J.I. & Turner, T.J. Exocytotic Ca^{2+} channels in mammalian central neurons. *Trends Neurosci.* **18**, 89–98 (1995).
3. Zhang, J.F. *et al.* Distinctive pharmacology and kinetics of cloned neuronal Ca^{2+} channels and their possible counterparts in mammalian CNS neurons. *Neuropharmacol.* **32**, 1075–1088 (1993).
4. Wheeler, D.B., Randall, A. & Tsien, R.W. Roles of N-type and Q-type Ca^{2+} channels in supporting hippocampal synaptic transmission. *Science* **264**, 107–111 (1994).
5. West, A.E., Griffith, E.C. & Greenberg, M.E. Regulation of transcription factors by neuronal activity. *Nat. Rev. Neurosci.* **3**, 921–931 (2002).
6. Westenbroek, R.E., Ahlijanian, M.K. & Catterall, W.A. Clustering of L-type Ca^{2+} channels at the base of major dendrites in hippocampal pyramidal neurons. *Nature* **347**, 281–284 (1990).
7. Westenbroek, R.E. *et al.* Biochemical properties and subcellular distribution of an N-type calcium channel alpha 1 subunit. *Neuron* **9**, 1099–1115 (1992).
8. Westenbroek, R.E. *et al.* Immunochemical identification and subcellular distribution of the α_{1A} subunits of brain calcium channels. *J. Neurosci.* **15**, 6403–6418 (1995).
9. Cohen-Cory, S. The developing synapse: construction and modulation of synaptic structures and circuits. *Science* **298**, 770–776 (2002).
10. Garner, C.C., Zhai, R.G., Gundelfinger, E.D. & Ziv, N.E. Molecular mechanisms of CNS synaptogenesis. *Trends Neurosci.* **25**, 243–251 (2002).
11. Sheng, M. Molecular organization of the postsynaptic specialization. *Proc. Natl. Acad. Sci. USA* **98**, 7058–7061 (2001).
12. Nishimune, H., Sanes, J.R. & Carlson, S.S. A synaptic laminin-calcium channel interaction organizes active zones in motor nerve terminals. *Nature* **432**, 580–587 (2004).
13. Catterall, W.A. Interactions of presynaptic Ca^{2+} channels and snare proteins in neurotransmitter release. *Ann. NY Acad. Sci.* **868**, 144–159 (1999).
14. Chen, Y. *et al.* Formation of an endophilin-Ca^{2+} channel complex is critical for clathrin-mediated synaptic vesicle endocytosis. *Cell* **115**, 37–48 (2003).
15. Herlitze, S. *et al.* Targeting mechanisms of high voltage-activated Ca^{2+} channels. *J. Bioenerg. Biomembr.* **35**, 621–637 (2003).
16. Vallee, R.B., Williams, J.C., Varma, D. & Barnhart, L.E. Dynein: an ancient motor protein involved in multiple modes of transport. *J. Neurobiol.* **58**, 189–200 (2004).
17. Hirokawa, N. Kinesin and dynein superfamily proteins and the mechanism of organelle transport. *Science* **279**, 519–526 (1998).
18. Karcher, R.L., Deacon, S.W. & Gelfand, V.I. Motor-cargo interactions: the key to transport specificity. *Trends Cell Biol.* **12**, 21–27 (2002).
19. Vale, R.D. The molecular motor toolbox for intracellular transport. *Cell* **112**, 467–480 (2003).
20. Setou, M., Nakagawa, T., Seog, D.H. & Hirokawa, N. Kinesin superfamily motor protein KIF17 and mLin-10 in NMDA receptor-containing vesicle transport. *Science* **288**, 11796–11802 (2000).
21. Tai, A.W., Chuang, J.Z., Bode, C., Wolfrum, U. & Sung, C.H. Rhodopsin's carboxy-terminal cytoplasmic tail acts as a membrane receptor for cytoplasmic dynein by binding to the dynein light chain Tctex-1. *Cell* **97**, 877–887 (1999).
22. Maeno-Hikichi, Y. *et al.* A PKCε-ENH-channel complex specifically modulates N-type Ca^{2+} channels. *Nat. Neurosci.* **6**, 468–475 (2003).
23. King, S.M. *et al.* The mouse t-complex-encoded protein Tctex-1 is a light chain of brain cytoplasmic dynein. *J. Biol. Chem.* **271**, 32281–32287 (1996).
24. Kamal, A. & Goldstein, L.S. Principles of cargo attachment to cytoplasmic motor proteins. *Curr. Opin. Cell Biol.* **14**, 63–68 (2002).
25. Llinas, R., Sugimori, M. & Silver, R.B. Microdomains of high calcium concentration in a presynaptic terminal. *Science* **256**, 677–679 (1992).
26. Williams, M.E. *et al.* Structure and functional expression of an ω-conotoxin-sensitive human N-type calcium channel. *Science* **257**, 389–395 (1992).
27. Gordon, G.W., Berry, G., Liang, X.H., Levine, B. & Herman, B. Quantitative fluorescence resonance energy transfer measurements using fluorescence microscopy. *Biophys. J.* **74**, 2702–2713 (1998).
28. Jiang, X. & Sorkin, A. Coordinated traffic of Grb2 and Ras during epidermal growth factor receptor endocytosis visualized in living cells. *Mol. Biol. Cell.* **13**, 1522–1535 (2002).
29. Siegel, R.M. *et al.* Measurement of molecular interactions in living cells by fluorescence resonance energy transfer between variants of the green fluorescent protein. *Sci. STKE* **2000**, PL1 (2000).
30. Erickson, M.G., Alseikhan, B.A., Peterson, B.Z. & Yue, D.T. Preassociation of calmodulin with voltage-gated Ca^{2+} channels revealed by FRET in single living cells. *Neuron.* **31**, 973–985 (2001).
31. Dotti, C., Sullivan, C. & Banker, G. The establishment of polarity by hippocampal neurons in culture. *J. Neurosci.* **8**, 1454–1468 (1988).
32. Bartlett, W. & Banker, G. An electron microscopic study of the development of axons and dendrites by hippocampal neurons in culture. II. Synaptic relationships. *J. Neurosci.* **4**, 1954–1965 (1984).
33. Pravettoni, E. *et al.* Different localizations and functions of L-type and N-type calcium channels during development of hippocampal neurons. *Dev. Biol.* **227**, 581–594 (2000).
34. Jones, O.T. *et al.* N-type calcium channels in the developing rat hippocampus: subunit, complex, and regional expression. *J. Neurosci.* **17**, 6152–6164 (1997).
35. Bahls, F.H. *et al.* Contact-dependent regulation of N-type calcium channel subunits during synaptogenesis. *J. Neurobiol.* **35**, 198–208 (1998).
36. Maximov, A. & Bezprozvanny, I. Synaptic targeting of N-type calcium channels in hippocampal neurons. *J. Neurosci.* **22**, 6939–6952 (2002).
37. King, S.M. *et al.* Cytoplasmic dynein contains a family of differentially expressed light chains. *Biochem.* **37**, 15033–15041 (1998).
38. Fuhrmann, J.C. *et al.* Gephyrin interacts with dynein light chains 1 and 2, components of motor protein complexes. *J. Neurosci.* **22**, 5393–5402 (2002).
39. Schwarzer, C., Barnikol-Watanabe, S., Thinnes, F.P. & Hilschmann, N. Voltage-dependent anion-selective channel (VDAC) interacts with the dynein light chain Tctex1 and the heat-shock protein PBP74. *Int. J. Biochem. Cell Biol.* **34**, 1059–1070 (2002).
40. Nagano, F. *et al.* Interaction of Doc2 with tctex-1, a light chain of cytoplasmic dynein. Implication in dynein-dependent vesicle transport. *J. Biol. Chem.* **273**, 30065–30068 (1998).
41. Yano, H. *et al.* Association of Trk neurotrophin receptors with components of the cytoplasmic dynein motor. *J. Neurosci.* **21**, RC125 (2001).
42. Campbell, K.S., Cooper, S., Dessing, M., Yates, S. & Buder, A. Interaction of p59fyn kinase with the dynein light chain, Tctex-1, and colocalization during cytokinesis. *J. Immunol.* **161**, 1728–1737 (1998).
43. Mok, Y.K., Lo, K.W. & Zhang, M. Structure of Tctex-1 and its interaction with cytoplasmic dynein intermediate chain. *J. Biol. Chem.* **276**, 14067–14074 (2001).
44. Susalka, S.J., Hancock, W.O. & Pfister, K.K. Distinct cytoplasmic dynein complexes are transported by different mechanisms in axons. *Biochim. Biophys. Acta.* **1496**, 76–88 (2000).
45. Tai, A.W., Chuang, J.Z. & Sung, C.H. Localization of Tctex-1, a cytoplasmic dynein light chain, to the Golgi apparatus and evidence for dynein complex heterogeneity. *J. Biol. Chem.* **273**, 19639–19649 (1998).
46. Chuang, J.Z., Milner, T.A. & Sung, C.H. Subunit heterogeneity of cytoplasmic dynein: Differential expression of 14 kDa dynein light chains in rat hippocampus. *J. Neurosci.* **21**, 5501–5512 (2001).
47. Augustine, G.J. How does calcium trigger neurotransmitter release? *Curr. Opin. Neurobiol.* **11**, 320–326 (2001).
48. Rizo, J. & Sudhof, T.C. Snares and Munc18 in synaptic vesicle fusion. *Nat. Rev. Neurosci.* **3**, 641–653 (2002).
49. Gundelfinger, E.D., Kessels, M.M. & Qualmann, B. Temporal and spatial coordination of exocytosis and endocytosis. *Nat. Rev. Mol. Cell Biol.* **4**, 127–139 (2003).
50. Verhage, M. *et al.* DOC2 proteins in rat brain: complementary distribution and proposed function as vesicular adapter proteins in early stages of secretion. *Neuron* **18**, 453–461 (1997).